6

CERAMIC IMPLANT MATERIALS

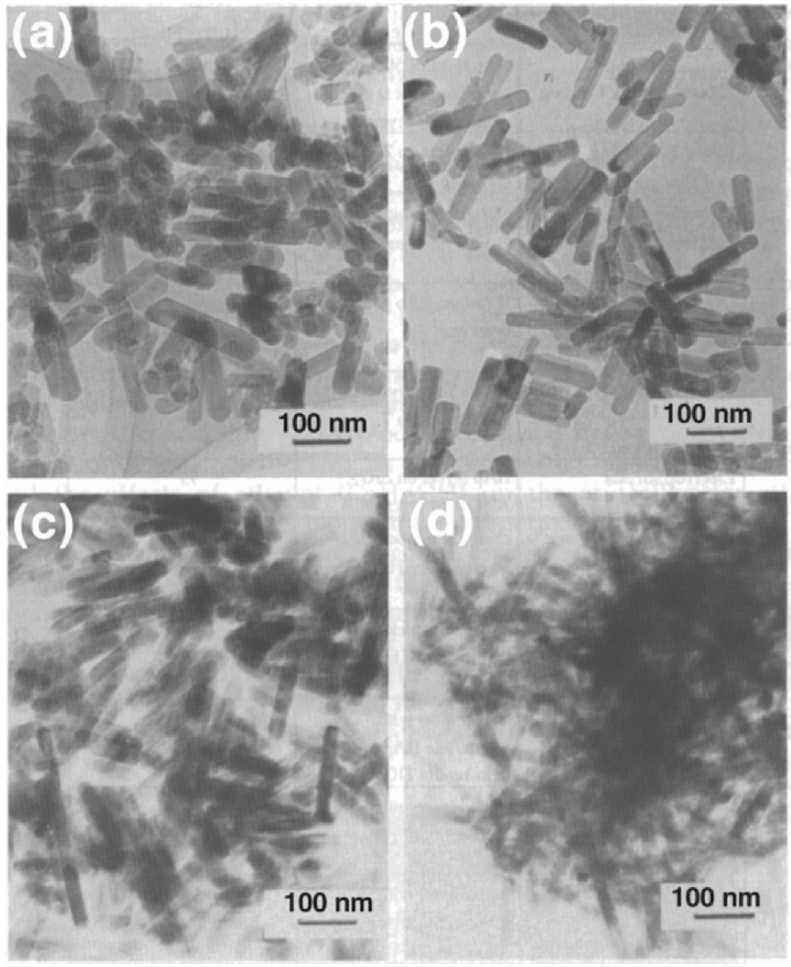

TEM photographs of hydroxyapatite crystals synthesized hydrothermally at 200ºC under 2 MPa for 5 hr: (**a**) without additives, (**b**) KOH (10 wt%) added, (**c**) K_3PO_4 (10 wt%) added, and (**d**) EDTA (5 wt%) added. Reprinted with permission from Yoshimura and Suda (1994). Copyright © 1994, Chemical Rubber Co.

Ceramics are refractory, polycrystalline compounds, usually inorganic, including silicates, metallic oxides, carbides, and various refractory hydrides, sulfides, and selenides. Oxides such as Al_2O_3, MgO, SiO_2, etc. contain metallic and nonmetallic elements. Ionic salts (NaCl, CsCl, ZnS, etc.) can form polycrystalline aggregates, but soluble salts are not suitable for structural biomaterials. Diamond and carbonaceous structures like graphite and pyrolized carbons are covalently bonded. The important factors influencing the structure and property relationship of the ceramic materials are radius ratios (§2.2.2) and the relative *electronegativity* between positive and negative ions.

Recently ceramic materials have been given a lot of attention as candidates for implant materials since they possess some highly desirable characteristics for some applications. Ceramics have been used for some time in dentistry for dental crowns by reason of their inertness to body fluids, high compressive strength, and good aesthetic appearance in their resemblance to natural teeth.

Some carbons have also found use as implants, especially for blood interfacing applications such as heart valves. Due to their high specific strength as fibers and their biocompatibility, they are also being used as a reinforcing component for composite implant materials and tensile loading applications such as artificial tendon and ligament replacements. Although the black color can be a drawback in some dental applications, this is not a problem if they are used as implants. They have such desirable qualities as good biocompatibility and ease of fabrication.

6.1. STRUCTURE–PROPERTY RELATIONSHIP OF CERAMICS

6.1.1. Atomic Bonding and Arrangement

As discussed earlier in Chapter 2 (Horwitz et al., 1993), when atoms such as sodium (metal) and chlorine (nonmetal) are ionized, the sodium will lose an electron and the chlorine will gain an electron:

$$\mathrm{Na} \Leftrightarrow \mathrm{Na}^{+} + e^{-}, \qquad e^{-} + \mathrm{Cl} \Leftrightarrow \mathrm{Cl}^{-}. \tag{6-1}$$

Thus, the sodium and chlorine can make an ionic compound by the strong affinity of the positive and negative ions. Again, soluble salts are not suitable for structural biomaterials. The negatively charged ions are much larger than the positively charged ions due to the gain and loss of electrons, as given in Table 6-1. The radius of an ion varies according to the coordination numbers: the higher the coordination number, the larger the radius. For example, the oxygen ion (O^{2-}) has a radius of 0.128, 0.14, and 0.144 nm for coordination numbers 4, 6, and 8, respectively.

Table 6-1. Atomic and Ionic Radii of Some Elements

	Group I			Group II			Group IV			Group VI	
Element	Atomic radius[a]	Ionic radius	Ele.	Atomic radius[a]	Ionic radius	Ele.	Atomic radius[a]	Ionic radius	Ele.	Atomic radius[a]	Ionic radius
Li^{+}	0.152	0.068	Be^{++}	0.111	0.031	O^{--}	0.074	1.40	F^{-}	0.071	0.130
Na^{+}	0.186	0.095	Mg^{++}	0.160	0.065	S^{--}	0.102	1.84	Cl^{-}	0.099	0.181
K^{+}	0.227	0.133	Ca^{++}	0.197	0.099	Se^{--}	0.116	1.98	Br^{-}	0.114	0.195

[a] Covalent. Units are in nm. Reprinted with permission from Starfield and Shrager (1972). Copyright © 1972, McGraw-Hill.

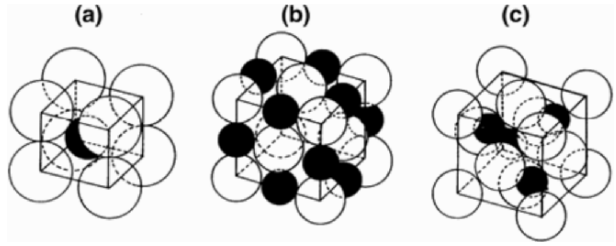

Figure 6-1. AX structures of ceramics. The dark spheres represent positive ions (A^+) and the circled ones represent negative ions (X^-).

Table 6-2. Selected A_mX_n Structures

Prototype compound	Lattice of A (or X)	CN of A (or X) sites	Available sites filled	Minimum r_A/R_x	Other compounds
CsCl	Simple cubic	8	All	0.732	CsI
NaCl	fcc	6	All	0.414	MgP, MnS, LiF
ZnS	fcc	4	1/2	0.225	β-SiC, CdS, AlP
Al_2O_3	hcp	6	2/3	0.414	Cr_2O_3, Fe_2O_3

Ceramics can be classified according to their structural compounds, of which A_mX_n is an example. The A represents a metal and X represents a nonmetal element, and *m* and *n* are integers. The simplest case of this system is the AX structure, of which there are three types (see Figure 6-1). The difference between these structures is due to the relative size of the ions (*minimum radius ratio*). If the positive and negative ions are about the same size ($r_A/R_X > 0.732$), the structure becomes a simple cubic (CsCl structure). A face-centered cubic structure arises if the relative sizes of the ions are quite different since the positive ions can be fitted in the tetragonal or octagonal spaces created among larger negative ions. These are summarized in Table 6-2. The aluminum and chromium oxide belong to the A_2X_3 type structure. The O^{2-} ions form hexagonal close packing, while the positive ions (Al^{3+}, Cr^{3+}) fill in 2/3 of the octahedral sites, leaving 1/3 vacant.

6.1.2. Physical Properties

Ceramics are generally hard; in fact, the measurement of hardness is calibrated against ceramic materials. Diamond is the hardest, with a hardness index on the Mohs scale of 10, and talc ($Mg_3Si_4O_{10}COH$) is the softest (Moh's hardness 1), and others such as alumina (Al_2O_3; hardness 9) quartz (SiO_2; hardness 8) and apatite (e.g., fluorapatite, $Ca_5P_3O_{12}F$; hardness 5) are in between. Other characteristics of ceramic materials are their high melting temperatures and low conductivity of electricity and heat. These characteristics come about as a result of the nature of the chemical bonding in ceramics.

Unlike metals and polymers, ceramics are difficult to shear plastically due to the ionic nature of bonding, as shown in Figure 6-2. In order to shear, the planes of atoms should slip past each other. However, for ceramic materials the ions with the same electric charge repel each

other; hence moving the plane of atoms is very difficult. This makes the ceramics brittle (non-ductile); moreover, creep at room temperature is almost zero. Some ceramics such as covalently bonded diamond have similar properties as those of ionic ceramics due to the breakages of theses primary bonds when deformed beyond their elastic limit. The ceramics are also very sensitive to notches or microcracks since instead of undergoing plastic deformation (or yield) they will fracture elastically once the crack propagates. This is also the reason why the ceramics have low tensile strength compared to the compressive strength, as discussed in §3.1.2. If the ceramic is made flaw free, then it becomes very strong even in tension. Glass fibers made this way have tensile strengths twice that of a high-strength steel (≈7 GPa).

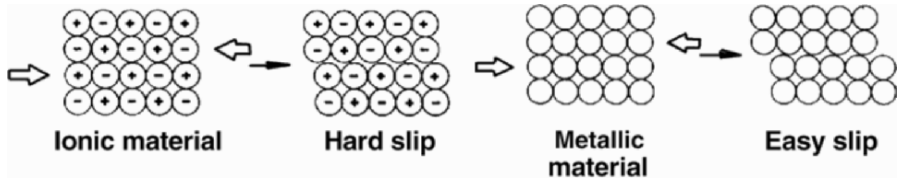

Figure 6-2. Schematic two-dimensional illustration of slips in ionic and non-ionic bond materials.

Example 6-1

A piece of window glass fails at 70 MPa (10^4 psi). Calculate the largest size elliptic crack which is responsible for the low strength. The stress concentration factor (σ/σ_a) can be expressed as $2\sqrt{c/r}$, where c is the crack depth ($2c$ if away from surface) and r is the crack tip radius.

Answer

Assuming the crack tip radius has the dimension of an oxygen ion (0.14 nm) and the theoretical strength of glass is 7 GPa,

$$c = \frac{r(\sigma/\sigma_a)^2}{4}$$
$$= \frac{(1.4)(7000/70)^2}{4}$$
$$= \underline{3.5 \times 10^2 \text{ nm or } 0.35\ \mu\text{m}}.$$

So, even a small microcrack significantly weakens the glass.

6.2. ALUMINUM OXIDES (ALUMINA)

Alpha-alumina (α-Al_2O_3) has a hexagonal close-packed structure (a = 0.4758 nm and c = 1.2991 nm). Natural alumina is known as sapphire or ruby (depending on the types of impurities that give rise to color). The single-crystal form of alumina has been used successfully to make implants. Single-crystal alumina can be made by feeding fine alumina powders onto the surface of a seed crystal, which is slowly withdrawn from an electric arc or oxy-hydrogen

flame as the fused powder builds up. Alumina single crystals up to 10 cm in diameter have been grown by this method.

The main source of high-purity alumina (aluminum oxide) is bauxite and native corundum. The commonly available (alpha, α) alumina can be prepared by calcining alumina trihydrate resulting in calcined alumina. The chemical composition and density of commercially available "pure" calcined alumina are given in Table 6-3. The American Society for Testing and Materials (ASTM) specifies 99.5% pure alumina and less than 0.1% of combined SiO_2 and alkali oxides (mostly Na_2O) for implant use.

Table 6-3. Chemical Composition of Calcined Aluminas

Chemicals	Composition (weight %)
Al_2O_3	99.6
SiO_2	0.12
Fe_2O_3	0.03
Na_2O	0.04

Aluminum Company of America. Reprinted with permission from Gitzen (1970). Copyright © 1970, American Ceramic Society.

Table 6-4. Physical Property Requirements of Alumina Implants (ASTM, 2000)

Properties	Values
Flexural strength	> 400 MPa (58,000 psi)
Elastic modulus	380 GPa (55.1×10^6 psi)
Density (g/cm^3)	3.8–3.9

The strength of polycrystalline alumina depends on porosity and grain size. Generally the smaller the grains and porosity, the higher the resulting strength. The ASTM standards (F603-78) require a flexural strength of greater than 400 MPa and an elastic modulus of 380 GPa, as given in Table 6-4.

Alumina in general is a quite hard material (Mohs number of 9); the hardness varies from 2,000 kg/mm^2 (19.6 GPa) to 3,000 kg/mm^2 (29.4 GPa). This high hardness permits one to use alumina as an abrasive (emery) and as bearings for watch movements. The high hardness is accompanied by low friction and wear; these are major advantages of using the alumina as joint replacement material in spite of its brittleness.

6.3. ZIRCONIUM OXIDES (ZIRCONIA)

Zirconium oxides or zirconia (ZrO_2) have been tried for application in fabricating implants. Zirconia is called "fake diamond" or "cubic zirconia" since it has a high refractive index (as does diamond) and some zirconia single crystals can be made gem grade. Some mechanical properties are as good or better than alumina ceramics. Zirconia is highly biocompatible, as are other ceramics, and can be made in the form of large implants such as the femoral head and acetabular cup in total hip joint replacement. These materials are strengthened by phase trans-

formation and control of grain sizes. A major drawback is that they may be weakened significantly under stress in the presence of moisture; this weakening occurs at a much faster rate at elevated temperature such as occurs during steam sterilization (autoclaving).

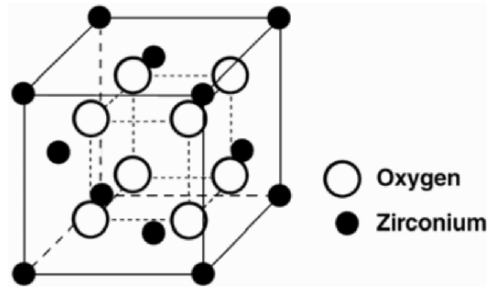

Figure 6-3. Cubic structure of zirconia that belongs to the fluorite structure. Modified with permission from Kingery et al. (1976). Copyright © 1976, Wiley.

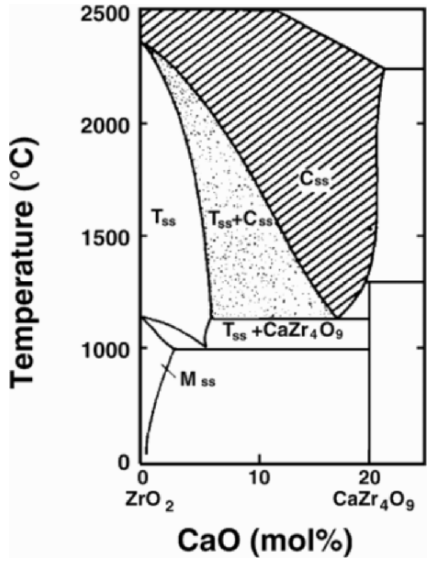

Figure 6-4. Partial phase diagram of ZrO_2–CaO: C_{ss} denotes cubic, T_{ss} tetragonal, and M_{ss} monoclinic solid solution phase. Reprinted with permission from Drennan and Steele (1986). Copyright © 1986, Pergamon Press.

6.3.1. Structure of Zirconia

The zirconia is allotropic and the transition from monoclinic ($a \neq b \neq c$, $\alpha = \gamma = 90 \neq \beta$) to tetragonal ($a = b \neq c$, $\alpha = \gamma = \beta = 90°$) at 1000~1200ºC and tetragonal to cubic ($a = b = c$, $\alpha = \gamma = \beta = 90°$) structure at 2370ºC. The monoclinic-to-tetragonal phase transition is a diffusionless transformation accompanying a volume reduction of 7.5%. The cubic structure of the zirconia belongs to the fluorite (CaF_2) structure, as shown in Figure 6-3. The crystallographic parameters of the unit cell structures are given in Table 6-5. The partial phase diagram of

Table 6-5. Physical Properties of Zirconia

Property	Values
Polymorphism[a,b]	
Monoclinic tetragonal	1273–1473 (K)
Tetragonal cubic	2643 (K)
Cubic liquid	2953 (K)
Crystallography	
Monoclinic	
a	5.1454 Å
b	5.2075 Å
c	5.3107 Å
	99°14'
Space group	$P2_1/c$
Tetragonal	
a	3.64 Å[c]
c	5.27 Å
Space group	$P4_2/nmc$
Cubic	
a	5.065 Å
Space group	Fm3m
Density (g/cm^3)	
Monoclinic	5.6
Tetragonal	6.10
Cubic	6.29[a]
Thermal expansion coefficient[c] (10^{-6}/K)	
Monoclinic	7
Tetragonal	12
Heat of formationc (kJ/mol)	–1096.7
Boiling point (K)	4549
Thermal conductivity (W /m/K)	
at 100ºC	1.675
at 1300ºC	2.094
Mohs hardness	6.5
Refractive index	2.15

[a] Calculated value (see Ex. 6-2).

ZrO_2–CaO is shown in Figure 6-4. The CaO acts as a stabilizing oxide, where Css is the cubic solid solution, called fully stabilized zirconia, which is resistant to most molten metals; thus it is used to make crucibles. Partially stabilized zirconia (PSZ) is resulted in the two-phase region of [Tss + Css]. These materials have enhanced mechanical properties. Another oxide commonly used to stabilize cubic zirconia is yttrium oxide (Y_2O_3), as shown in Figure 6-5. It is critical that the precipitates of tetragonal phase remain small (<0.2 μm) in the cubic zirconia matrix to enhance its mechanical properties. If the tetragonal precipitates become large the phase transforms into monoclinic, causing cracks in the material. To control the phase transformation MgO is used along with Y_2O_3 during sintering and the aging process. Figure 6-6 shows the microstructures of yttrium- and magnesium-stabilized zirconia. The tetragonal precipitates strengthen the structure of the cubic zirconia matrix due to the volume difference during the phase transformation.

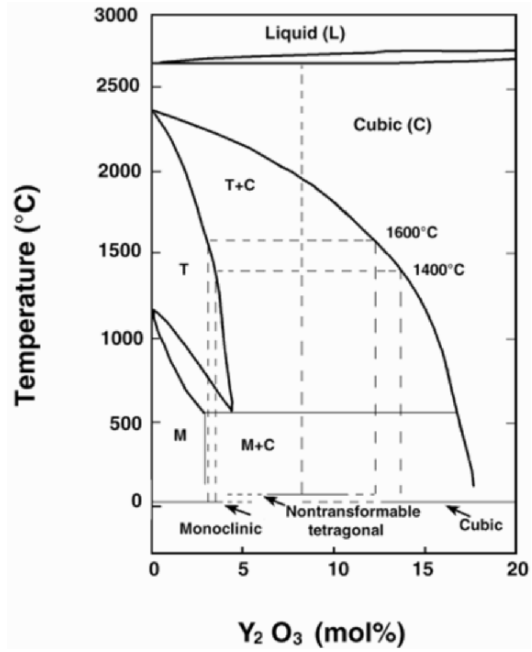

Figure 6-5. Phase diagram of ZrO_2–Y_2O_3. Reprinted with permission from Burger and Willmann (1993). Copyright © 1993, Pergamon Press.

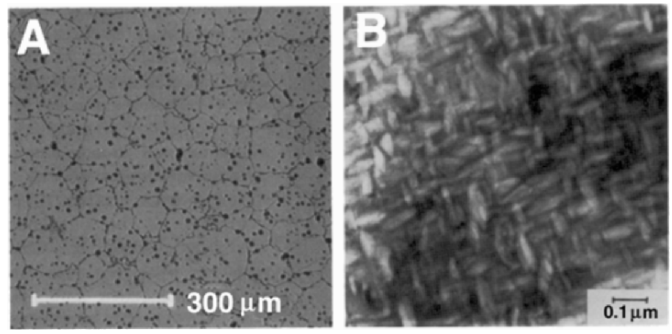

Figure 6-6. Yttria- and magnesium-stabilized zirconia (**A**) and tetragonal precipitates (**B**) in cubic matrix grains. Reprinted with permission from Burger and Willmann (1993). Copyright © 1993, Pergamon Press.

6.3.2. Properties of Zirconia

Properties of various zirconia are summarized in Table 6-6. The strength data for the partially stabilized zirconia with yttrium oxide showed the highest flexural strength and fracture toughness. However, the Weibull modulus was lower than the yttrium magnesium oxide-stabilized

Table 6-6. Properties of Various Zirconia

Properties	CSZ	Y–Mg–PSZ	Y-TZP
Young's modulus (GPa)	210	210	210
Flexural strength (MPa)	200	600	950
Hardness (Vickers, HV0.5)	1250	1250	1250
Fracture toughness (MPa $m^{1/2}$)	–	5.8	10.5
Weibull modulus	8	25	18
Density	6.1	5.85	6

Reprinted with permission from Burger and Willmann (1993). Copyright © 1983, Pergamon.

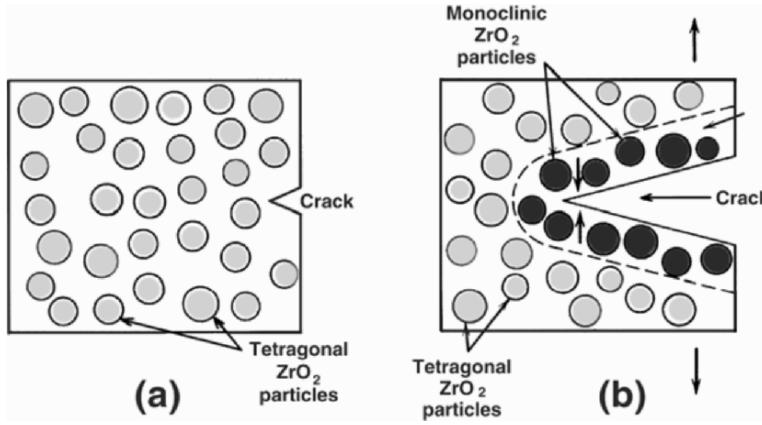

Figure 6-7. Schematic representation of the toughening of zirconia with partially stabilized zirconia: (**a**) crack before phase transformation; (**b**) crack arrestment due to phase transformation of the dispersed PSZ particles. Reprinted with permission from Callister (1994). Copyright © 1994, Wiley.

zirconia. It is also interesting that the increased fracture toughness is due to a phase transformation that operates by arresting the propagation of cracks, as shown in Figure 6-7. Small particles of partially stabilized ZrO_2 are dispersed in the matrix materials, which could be zirconia itself. This partial stabilization enables the retention of a metastable tetragonal structure at ambient temperature. During crack propagation the tetragonal particles in the crack tip region undergo phase transformation, increasing its volume, which sets up a compressive field surrounding the particles and closes the crack opening, resulting in a stronger material. The process is similar to the precipitation of a tetragonal structure in cubic grains.

The yttrium-stabilized zirconia has been used for fabricating the femoral head of total hip joint prostheses and has two advantages over the alumina. One is the finer grain size and a well-controlled microstructure without any residual porosity of the Y-TZP, making it better tribological material than the alumina. The other is higher fracture strength and toughness due to the phase transformation toughening process.

As mentioned, zirconia has many salient features in comparison with alumina. A comparison of the properties is given in Table 6-7. The biocompatibility of zirconia is about the same as alumina ceramic, but its tribological properties are quite different. In one study the friction

and wear properties of zirconia, alumina, and 316L stainless steel against ultra-high-molecular-weight polyethylene (UHMWPE) were evaluated by using a uni- and bidirectional wear testing machine in bovine serum, saline, and distilled water. Table 6-8 shows the results of wear of UHMWPE. The wear factor was estimated by the following equation:

$$\text{Wear factor} = \frac{\text{Wear volume } (\text{mm}^3)}{\text{Load (N)/Sliding distance (m)}}. \quad (6\text{-}2)$$

Table 6-7. Comparison of Properties of Alumina and Zirconia

Property	Alumina	Zirconia
Chemical composition	$A1_20_3$ + MgO	ZrO_2 + MgO + Y_20_3
Purity (%)	99.9	95~97
Density (g/cm^3)	> 3.97	5.74~6.0
Porosity (%)	< 0.1	< 0.1
Bending strength (MPa)	> 500	500~1 000
Compression strength (MPa)	4100	2000
Young's modulus (GPa)	380	210
Poisson's ratio	0.23	0.3
Fracture toughness (MPa m$^{1/2}$)	4	up to 10
Thermal expansion coefficient ($\times 10^{-6}$/K)	8	11
Thermal conductivity (W/m/K)	30	2
Hardness (HV0. 1)	up to 2200	1200
Contact angle (°)	10	50

Reprinted with permission from Willmann (1993). Copyright © 1993, Pergamon.

Table 6-8. Wear of UHMWPE on Two Different Wear Devices

	*Wear factor (mm^3/N-m) $\times 10^{-9}$					
Medium	Bovine serum		Saline		Distilled water	
Counterfaces	Unidirectional	Reciprocate	Unidirectional	Reciprocate	Unidirectional	Reciprocate
Zirconia (3)	10.7 ± 12	0.56 ± 14	7.5 ± 3	0.45 ± 5	8.61 ± 11	0.38 ± 6
Alumina (3)	18.2 ± 6	1.01 ± 8	32.7 ± 7	0.57 ± 2	11.8 ± 4	0.68 ± 4
316L SS (2)	27.7 ± 30	1.81 ± 4	90.5 ± 40	3.89 ± 8	37.1 ± 10	1.12 ± 10

( ) = number of specimens tested. *Average and range.
Reprinted with permission from Kumar et al. (1991). Copyright © 1991, Wiley.

The wear factor for the yttrium oxide-stabilized (Y-PSZ) zirconia showed a smaller value to alumina and 316L stainless steel in all test conditions and modes. Also, the unidirectional wear test showed a greatly higher wear volume than the bidirectional (reciprocating) tests. The actual wear volume versus number of cycles in unidirectional tests is shown in Figure 6-8. The wear factor is the slope of the curve divided by the load (3.45 MPa).

The friction coefficient also showed a lower value for the zirconia (0.028–0.082) than alumina (0.044–0.115) or 316L stainless steel (0.061–0.156). As with the wear factor, the bidirectional reciprocating mode showed somewhat lower friction than the unidirectional arrangement, although it was not as drastic as for wear. Also, the types of lubricant did not influence the friction. One reason for the excellent wear and friction characteristic of the zirconia is attributed to the fact that zirconia has less porosity, as shown in Figure 6-9. Also, the average

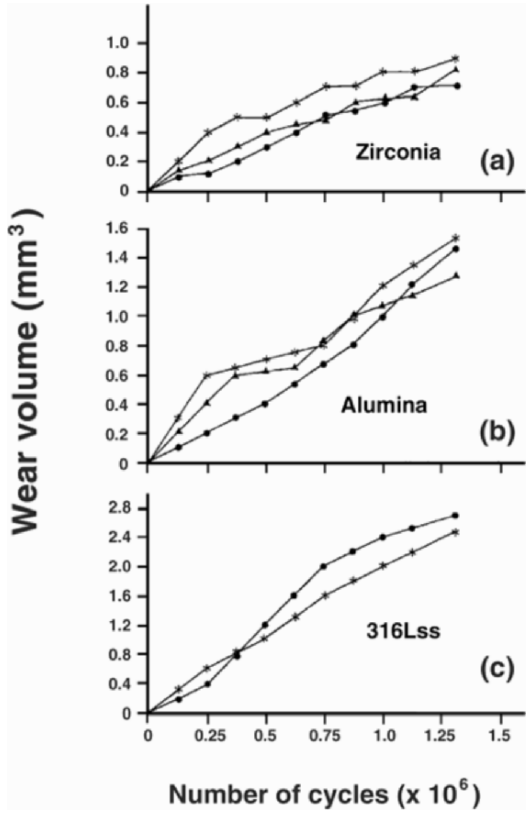

Figure 6-8. Wear volume versus number of cycles for unidirectional test (one cycle = 50 mm) for zirconia (**a**), alumina (**b**), and 316L stainless steel (**c**). Reprinted with permission from Kumar et al. (1991). Copyright © 1991, Wiley.

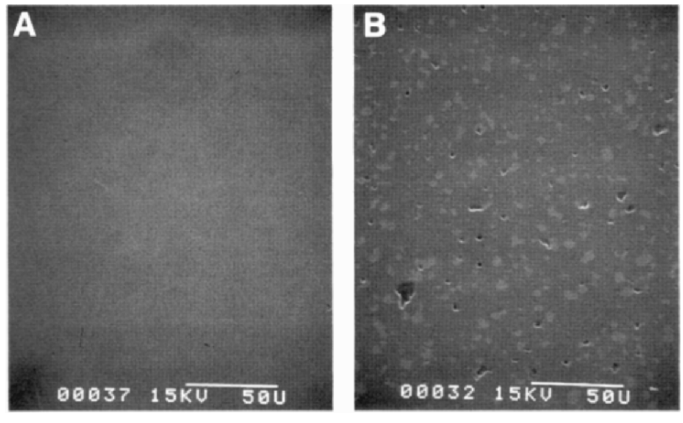

Figure 6-9. Scanning electron microscopic picture of polished surfaces of zirconia (**A**) and alumina (**B**). Note the porosity in the alumina. Reprinted with permission from Kumar et al. (1991). Copyright © 1991, Wiley.

grain size of zirconia (0.3 μm) was about one-tenth that of the alumina (2.5 μm), although the surface roughness was about the same for both (0.005–0.013 μm R_a, the average root mean square value of surface roughness).

Some researchers evaluated the use of zirconia for a hemiarthroplasty femoral head implant and found it suitable due to its low friction with articular cartilage and its excellent biocompatibility. On the other hand, the wear rate of zirconia–zirconia is many times that of the alumina–alumina combination, preempting its use for the femoral head and socket.

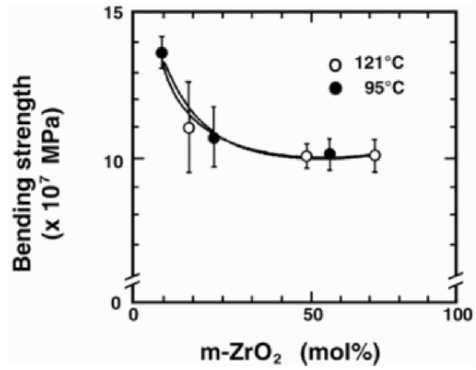

Figure 6-10. Relationship between the bending strength and amount of phase transformation aged in water at 95 and 121ºC. Reprinted with permission from Shimizu et al. (1993). Copyright © 1993, Wiley.

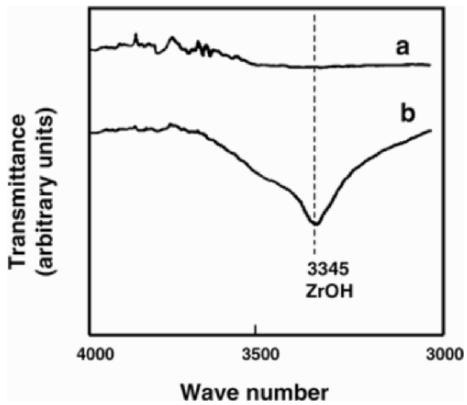

Figure 6-11. Fourier transform IR spectroscopy of zirconia before (**a**) and after (**b**) aging in water at 121ºC for 960 hr. Reprinted with permission from Shimizu et al. (1993). Copyright © 1993, Wiley.

There is a direct one-to-one relationship between the amount of phase transformation and bending strength of zirconia, as shown in Figure 6-10, indicating that only the amount of phase transformation influences the mechanical properties. The moisture has an effect on the zirconia by forming Zr–OH bonding that precedes the phase transformation and was detected by infrared (IR) spectroscopy, as shown in Figure 6-11. The yttria-stabilized zirconia is a good candi-

date to replace the alumina ceramic for orthopedic applications in spite of the effect of aging on the mechanical properties on zirconia. Even after aging, zirconia is a much stronger material than alumina, which has a strength of about 400 MPa.

Example 6-2

Calculate the density of cubic zirconia and compare that with the other forms of zirconia given in Table 6.5.

Answer

$$\text{Density} = \frac{\text{Mass}}{\text{Volume}} = \frac{\left(4\times 91 + 8\times 16\right)\text{gmol}^{-1}}{\left(5.065\times 10^{-8}\text{cm}\right)^3\, 6.02\times 10^{23}\text{mol}^{-1}} = \underline{6.29\ \text{g/cm}^3}.$$

This value seems very reasonable compared to the density of the tetragonal structure, 6.10 g/cm^3. However, it is somewhat odd that the density increases with increased temperature since the cubic structure exists at higher temperature than the tetragonal zirconia.

6.3.3. Manufacture of Zirconia

Zircon ($ZrSiO_4$) is a gold-colored silicate of zirconium; zircon is a mineral (baddeleyite) found in igneous and sedimentary rocks and occurring in tetragonal crystals colored yellow, brown, or red, depending on impurities. The zircon is first chlorinated to form $ZrCl_4$ in a fluidized bed reactor in the presence of petroleum coke. A second chlorination is required for high-quality zirconium. Zirconium is precipitated with either hydroxides or sulfates, then calcined to its oxide.

The zirconia is partially stabilized above 1700ºC in the cubic phase, which results in large grain sizes (50-70 μm). When it is cooled, a phase transformation takes place and tetragonal precipitates can be formed in the cubic matrix. Combined cubic and tetragonal phase results in enhanced mechanical properties.

Example 6-3

Calculate the wear constant of UHMWPE with zirconia as a mating material for a joint replacement. Use the data in Figure 6-8.

Answer

From Figure 6-8, the average wear volume for zirconia in bovine serum is about 0.6 mm^3 after 10^5 cycles, with a sliding distance of 50 mm. Therefore, the wear constant can be calculated, since the wear constant is defined as (ΔV is wear volume, Δl is total sliding distance, P is load, and H is hardness)

$$\text{Wear constant } (K) = \frac{0.6\ \text{mm}^3 \times 3\times 100\ \text{MPa}}{43.35\ \text{N}\ \times 50\ \text{mm}\times 10^5} = \underline{8.3\ \times\ 10^{-7}}.$$

Assume the hardness of the UHMWPE is about 100 MPa, and the load applied 43.4 N. This corresponds to a stress of 3.45 MPa.

The wear constant for the UHMWPE with 316L stainless steel would be about 3 times larger according to the wear volume at 100,000 cycles(~2 mm^3)

6.4. CALCIUM PHOSPHATE

Calcium phosphate has been used to make artificial bone. Recently, this material has been synthesized and used for manufacturing various forms of implant as well as for solid or porous coatings on other implants. There are mono-, di-, tri-, and tetra-calcium phosphates, in addition to the hydroxyapatite and β-whitlockite, which have ratios of 5/3 and 3/2 for calcium and phosphorus (Ca/P), respectively. The stability in solution generally increases with increasing Ca/P ratios. Hydoxyapatite is the most important among the calcium compounds since it is found in natural hard tissues as mineral phase. Hydroxyapatite acts as a reinforcement in hard tissues and is responsible for the stiffness of bone, dentin, and enamel.

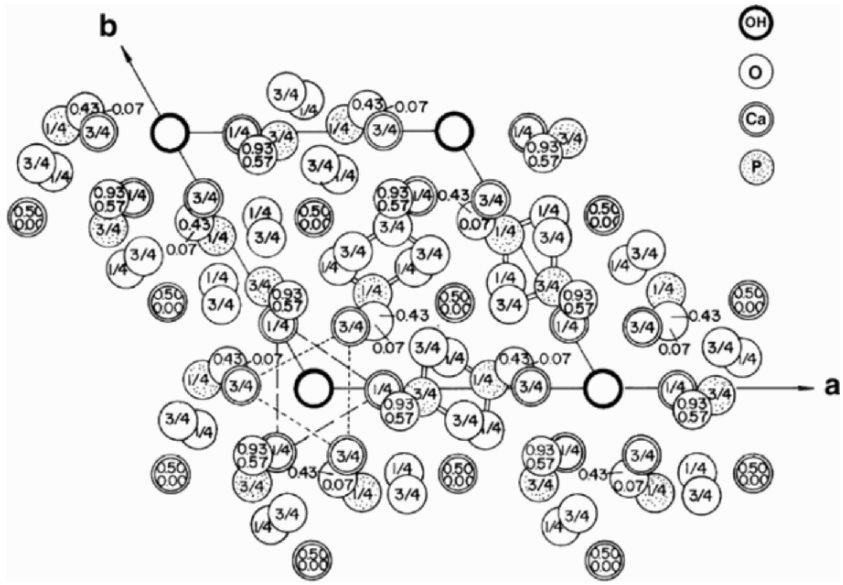

Figure 6-12. Hydroxyapatite structure projected down the *c*-axis on the basal plane. Reprinted with permission from Posner et al. (1958). Copyright © 1958, Munksgaard International.

6.4.1. Structure of Calcium Phosphate (Hydroxyapatite)

Calcium phosphate can be crystallized into the salts mono-, di- tri-, and tetra-calcium phosphate, hydroxyapatite, and β-whitlockite, depending on the Ca/P ratio, presence of water, impurities, and temperature. The most important is the hydroxyapatite due to its presence in natural bone and teeth. In a wet environment and at lower temperature (<900ºC), it is more likely that the (hydroxyl or hydroxy) apatite will form while in a dry atmosphere and at higher temperature the β-whitlockite ($3CaO{\cdot}P_2O_3$) will be formed. Both forms are very tissue compatible and are used for bone substitute in granular form or as a solid block. We will consider the apatite form of the calcium phosphate since it is considered more closely related to the mineral phase of bone and teeth.

The mineral part of bone and teeth is made of a crystalline form of calcium phosphate similar to hydroxyapatite [$Ca_{10}(PO_4)_6(OH)_2$]. The apatite family of minerals, $A_{10}(BO_4)_6X_2$, crys-

tallizes into hexagonal rhombic prisms and has unit cell dimensions a = 0.9432 nm and c = 0.6881 nm. The atomic structure of hydroxyapatite projected down on the c-axis onto the basal plane is given in Figure 6-12. Note that the hydroxyl ions lie on the corners of the projected basal plane, and they occur at equidistant intervals along half of the cell (0.344 nm), along columns perpendicular to the basal plane and parallel to the c-axis. Six of the ten calcium ions in the unit cell are associated with the hydroxyls in these columns, resulting in strong interactions.

The ideal Ca/P ratio of hydroxyapatite is 10/6 and the calculated density is 3.219 g/cm^3. It is interesting to note that the substitution of OH with F will give greater chemical stability due to the closer coordination of F (symmetric shape) as compared to the hydroxyl (nonsymmetric, two atoms) by the nearest calcium. This is one of the reasons for the better caries resistance of teeth following fluoridation.

6.4.2. Properties of Calcium Phosphates (Hydroxyapatite)

There is a wide variation of the mechanical properties of synthetic calcium phosphates, as given in Table 6-9. The wide variations of properties are due to the variations in the structure of polycrystalline calcium phosphates due to variations in the manufacturing processes. Depending on the final firing conditions, the calcium phosphate can be calcium hydroxyapatite or β–whitlockite. In many instances, however, both types of structure exist in the same final product.

Table 6-9. Physical Properties of Synthetic Calcium Phosphates

Properties	Values
Elastic modulus (GPa)	40–117
Compressive strength (MPa)	294
Bending strength (MPa)	147
Hardness (Vickers, GPa)	3.43
Poisson's ratio	0.27
Density (theoretical, g/cm^3)	3.16

And other sources.

Polycrystalline hydroxyapatite has a high elastic modulus (40–117 GPa). Hard tissues such as bone, dentin, and dental enamel are natural composites that contain hydroxyapatite (or a similar mineral) as well as protein, other organic materials, and water. Enamel is the stiffest hard tissue with an elastic modulus of 74 GPa, and it contains the most mineral. Dentin (E = 21 GPa) and compact bone (E = 12~18 GPa) contain comparatively less mineral. The Poisson's ratio for the mineral or synthetic hydroxyapatite is about 0.27, which is close to that of bone ($\approx$ 0.3).

Among the most interesting properties of hydroxyapatite as a biomaterial is its excellent biocompatibility. Indeed, it appears to form a direct chemical bond with hard tissues. In an experimental trial, new lamellar cancellous bone was formed around implanted hydroxyapatite granules in the marrow cavity of rabbits after 4 weeks, as shown in Figure 6-13.

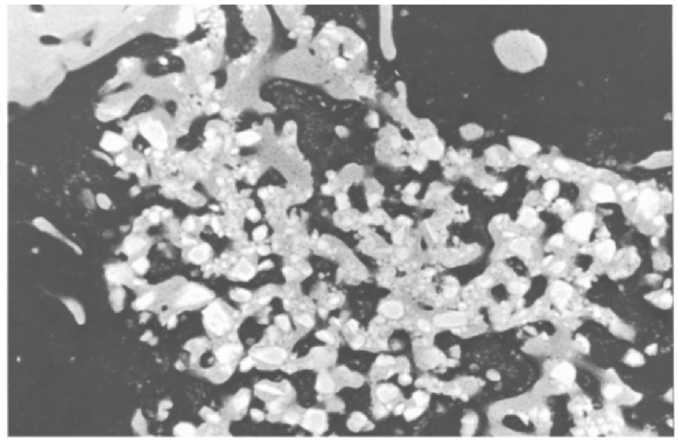

Figure 6-13. X-ray microradiographic picture showing the hydroxyapatite granules and bony tissues surrounding them after 4 weeks in a rabbit marrow cavity (40×). The mottled areas are regions of new bone deposition and the white areas are implants. Reprinted with permission from Niwa et al. (1980). Copyright © 1980, Springer-Verlag.

6.4.3. Manufacture of Calcium Phosphates (Hydroxyapatite)

Many different methods have been developed to make precipitates of hydroxyapatite from an aqueous solution of $Ca(NO_3)_2$ and NaH_2PO_4. One method uses precipitates that are filtered and dried to form a fine particle powder. After calcination for about 3 hours at 900ºC to promote crystallization, the powder is pressed into final form and sintered at about 1050–1200ºC for 3 hours. Above 1250ºC the hydroxyapatite shows a second phase precipitation along the grain boundaries.

Example 6-4

Calculate the theoretical density of hydroxyapatite crystal $[Ca_{10}(PO_4)_6(OH)_2]$.

Answer

From Figure 6-12 one can see that there are 10 Ca atoms in the hexagonal unit cell prism, 4 inside, (2 for 1/2, 2 for 1/4, 3/4 position), 2 for top and bottom (0 and 1 position), and 4 for sides (1/4, 3/4 position). Therefore,

$$\rho = \frac{(10\times 40 + 6\times 31 + 26\times 16 + 2\times 1)}{9.432\times\frac{\sqrt{3}}{2}\times 9.432\times 6.881\times 10^{-8}\times 6.01\times 10^{23}}$$

$$= \underline{3.16\ \text{g/cm}^3}.$$

(This is very close to the value given in the literature; McConell, 1963).

6.5. GLASS-CERAMICS

Glass-ceramics are polycrystalline ceramics made by controlled crystallization of glasses. They were originally developed by S.D. Stookey of Corning Glass Works in the early 1960s. They were first utilized in photosensitive glasses in which small amounts of copper, silver and gold are precipitated by ultraviolet light irradiation. These metallic precipitates help to nucleate and crystallize the glass into a fine grained ceramic which possess excellent mechanical and thermal properties. Bioglass® and Ceravital® are two glass-ceramics developed for implants.

6.5.1. Formation of Glass-Ceramics

The formation of glass-ceramics is influenced by the nucleation and growth of small (<1-μm diameter) crystals as well as the size distribution of these crystals. It is estimated that about 10^{12} to 10^{15} nuclei per cubic centimeter are required to achieve such small crystals. In addition to the metallic agents mentioned (Cu, Ag, and Au), Pt groups, TiO_2, ZrO_2, and P_2O_5 are widely used for this purpose. The nucleation of glass is carried out at temperatures much lower than the melting temperature. During processing the melt viscosity is kept in the range of 10^{11} and 10^{12} Poise for 1 to 2 hours. In order to obtain a larger fraction of the microcrystalline phase, the material is further heated to an appropriate temperature for maximum crystal growth. Deformation of the product, phase transformation within the crystalline phases, and redissolution of some of the phases are to be avoided. Crystallization is usually more than 90% complete with grain sizes of 0.1 to 1 μm. Grains smaller than one micron are called nanocrystalline. These grains are much smaller than those of the conventional ceramics. Figure 6-14 shows a schematic representation of the temperature–time cycle for a glass-ceramic.

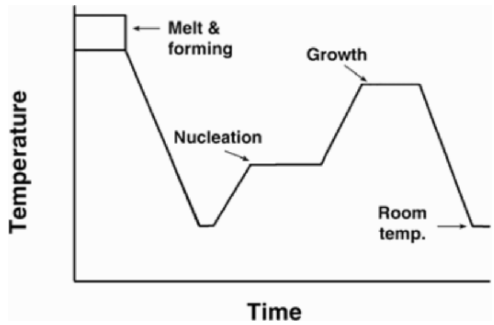

Figure 6–14. Temperature-time cycle for a glass ceramic. Reprinted with permission from Kingery et al. (1976). Copyright © 1976, Wiley.

The glass-ceramics developed for implantation are SiO_2–CaO–Na_2O–P_2O_5 and Li_2O–ZnO–SiO_2 systems. There are two different groups experimenting with the SiO_2–CaO–Na_2O–P_2O_5 glass-ceramic. One group varied the compositions (except for P_2O_5) as given in Table 6-10 in order to obtain the best composition to induce direct bonding with bone. The bonding is related to simultaneous formation of a calcium phosphate and an SiO_2-rich film layer on the surface, as exhibited by 46S5.2 type Bioglass®. If an SiO_2-rich layer forms first and a calcium phosphate film develops later (46–55 mol% SiO_2 samples) or no phosphate film is formed (60 mol% SiO_2), then no direct bonding with bone is observed. The approximate region of the SiO_2–CaO–Na_2O system for the tissue-glass ceramic reaction is shown in Figure 6-15. As can be seen, the best region (Region A) for good tissue bonding is the composition given for 46S5.2 type Bioglass® (Table 6-10).

Table 6-10. Compositions of Bioglass® and Ceravital® Glass-Ceramics

Type	Code	SiO_2	CaO	Na_2O	P_2O_5	MgO	K_2O
Bioglass							
	42S5.6	42.1	29.0	26.3	2.6	–	–
	(45S5)46S5.2	46.1	26.9	24.4	2.6	–	–
	49S4.9	49.1	25.3	23.0	2.6	–	–
	52S4.6	52.1	23.8	21.5	2.6	–	–
	55S4.3	55.1	22.2	20.1	2.6	–	–
	60S3.8	60.1	19.6	17.7	2.6	–	–
Cervital*							
	Bioactive	40.0–50.	30.0–35.0	5.0–10.0	10.0–15.0	2.5–5.0	0.5–3.0
	**Nonbioactive	30.0–35.0	25.0–30.0	3.5–7.5	7.5–12.0	1.0–2.5	0.5–2.0

*The Ceravital composition is in weight % while the Bioglass compositions are in mol %.

**In addition Al_2O_3 (5.0–15.0), TiO_2(1.0–5.0) and Ta_2O_5 (5.0–15.0) are added.

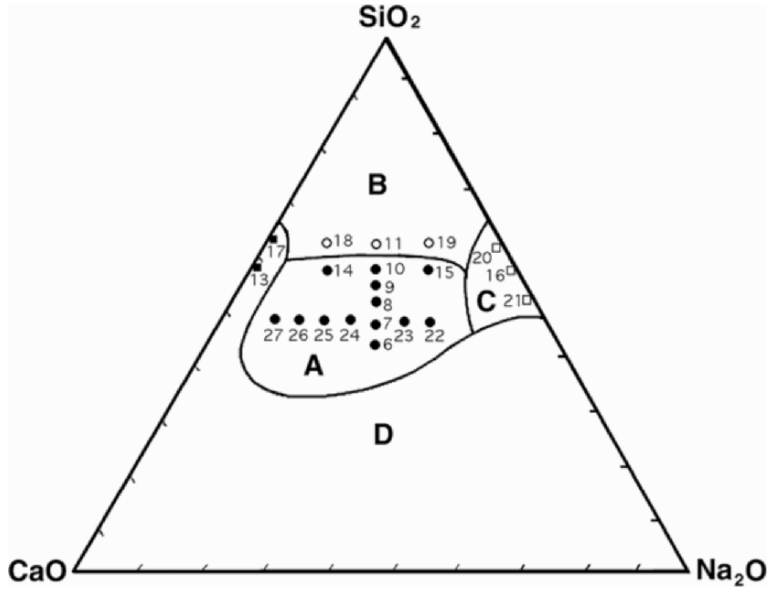

Figure 6-15. The SiO_2–CaO–Na_2O phase diagram. Region A: bonding in 30 days with bone. Region B: nonbonding—too low reactivity. Region C: nonbonding—too high reactivity. Region D: bonding but does not form glass. Reprinted with permission from Hench and Ethridge (1982). Copyright © 1982, Academic Press.

The composition of Ceravital® is similar to the Bioglass® in terms of SiO_2 content but differs somewhat in others, as given in Table 6-10. In addition, Al_2O_3, TiO_2, and Ta_2O_5 are used for the Ceravital® glass-ceramic in order to control the dissolution rate. The mixtures were melted in a platinum crucible at 1500ºC for 3 hours and annealed, and then cooled. The nuclea-

tion and crystallization temperatures were 680 and 750ºC, respectively, for 24 hours each. When the size of crystallites was about 0.4 nm and the crystals did not exhibit the characteristic needle structure, the process was stopped to obtain a fine grain structure.

6.5.2. Properties of Glass-Ceramics

Glass-ceramics have several desirable properties compared to glasses and ceramics. The thermal coefficient of expansion is very low, typically 10^{-7} to 10^{-5} per degree C, and in some cases it can be made even negative. Due to the controlled grain size and improved resistance to surface damage, the tensile strength of these materials can be increased by at least a factor of two, from about 100 to 200 MPa. The resistance to scratching and abrasion are close to that of sapphire.

In an experimental trial, Bioglass® glass-ceramic was implanted in the femur of rats for 6 weeks. Transmission electron micrographs showed intimate contacts between the mineralized bone and the Bioglass®, as given in Figure 6-16. The mechanical strength of the interfacial bond between bone and Bioglass® ceramic is the same order of magnitude as the strength of the bulk glass-ceramic (850 kg/cm^2 or 83.3 MPa), which is about three-fourths that of the host bone strength.

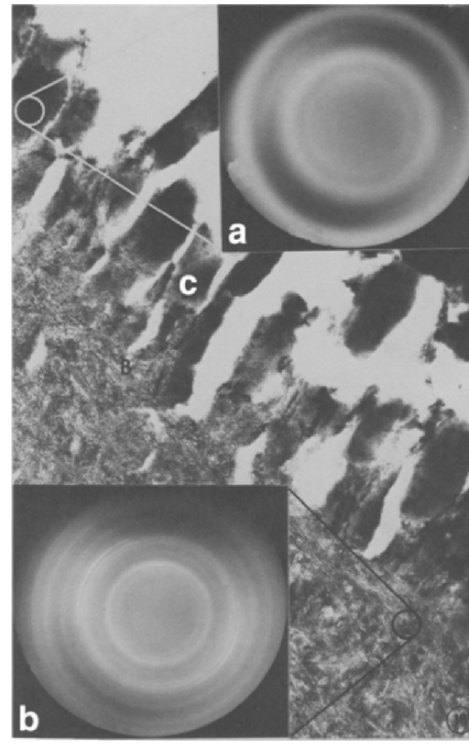

Figure 6-16. Transmission electron micrograph of well-mineralized bone (**b**) juxtaposed to the glass-ceramic (**c**), which was fractured during sectioning (×51,500). Insert (**a**) is the diffraction pattern from the ceramic area and (**b**) is from bone area. Reprinted with permission from Beckham et al. (1971). Copyright © 1971, Springer-Verlag.

The main drawback of the glass-ceramic is its brittleness, as is the case with other glasses and ceramics. Additionally, due to restrictions on the composition for biocompatibility (or osteogenicity), mechanical strength cannot be substantially improved as for other glass-ceramics. Therefore, they cannot be used for making major load-bearing implants such as joint implants. However, they can be used as fillers for bone cement, dental restorative composites, and coating material.

Example 6-5

From the phase diagram of Al_2O_3–SiO_2, answer the following:

a. Determine the exact w/o of Al_2O_3 for mullite, which has a $3Al_2O_3{\cdot}2Si0_2$ composition.

b. Determine the amount of liquid in 50 w/o Al_2O_3–50 w/o SiO_2 at 1588ºC.

Answer

a.

$$\frac{3Al_2O_3}{3Al_2O_3 + 2SiO_2} = \frac{6(27)+9\times16}{6\times27\times9\times16+2\times28+4\times16}$$

$$= \frac{162+144}{306+56+64}$$

$$= \frac{306}{426}$$

$$= \underline{0.718\ (71.8\%).}$$

b. Using the lever rule [see §5.1.1]:

$$\%L = \frac{71.8-50}{71.8-5.5} = \frac{21.8}{66.3} = \underline{0.329\ (32.9\%)}.$$

6.6. OTHER CERAMICS

There are many other ceramic materials studied as well, including titanium oxide (TiO_2), barium titanate ($BaTiO_3$), tricalcium phosphate ($Ca_3(PO_4)_2$), and calcium aluminate ($CaO{\cdot}Al_2O_3$). Titanium oxide was tried for use in a component of bone cement or as a blood-interfacing material. Porous calcium aluminate was used to induce tissue ingrowth into pores with the aim of achieving better implant fixation. However, this material loses its strength considerably after in vivo and in vitro aging, as shown in Figure 6-17. Tricalcium phosphate together with calcium aluminate were tried as biodegradable implants in the hope of regenerating new bone.

Barium titanate with a textured surface has been used in experimental trials to achieve improved fixation of implants to bone. This material is piezoelectric (following a polarization procedure). Therefore, mechanical loads on the implant will generate electrical signals that are capable of stimulating bone healing and ingrowth. These loads on the implant arise during use of the implanted limb. Alternatively, the implant can be exposed to ultrasound to generate electrical signals.

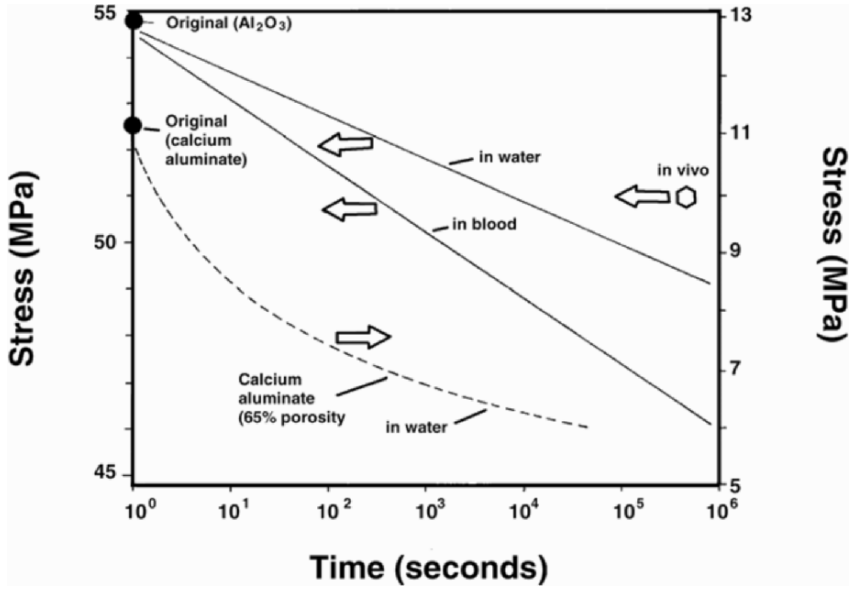

Figure 6-17. Aging effect on the strength of calcium aluminate in vitro and in vivo. Reprinted with permission from Schnittgrund et al. (1973). Copyright © 1973, Wiley.

6.7. CARBONS

Carbons can be made in many allotropic forms: crystalline diamond, graphite, noncrystalline glassy carbon, and partially crystalline (now referred to as icosahedral) pyrolytic carbon. Among these, only pyrolytic carbon is widely utilized for implant fabrication; it is normally used as a surface coating. It is also possible to coat surfaces with diamond-like carbon (DLC). This technique has the potential to improve performance of such medical devices as surgical knives, scissors, and articulating surfaces of joint implants; however, it is not, as of this writing, commercially available. This DLC coating is now used to coat razor blades.

6.7.1. Structure of Carbons

The crystalline structure of carbon as used in implants is similar to the graphite structure shown in Figure 6-18. The planar hexagonal arrays are formed by strong covalent bonds in which one valence electron per atom is free to move, resulting in high but anisotropic electric conductivity. The bonding between layers is stronger than the van der Waals force; therefore, *crosslinks* between them are considered to be present. Indeed, the remarkable lubricating property of graphite cannot be realized unless the crosslinks are eliminated.

The poorly crystalline carbons are thought to contain unassociated or unoriented carbon atoms. The hexagonal layers are not perfectly arranged, as shown in Figure 6-19. The strong bonding within layers and the weaker bonding between layers cause the properties of individual crystallites to be highly anisotropic. However, if the crystallites are randomly dispersed, then the aggregate becomes isotropic.

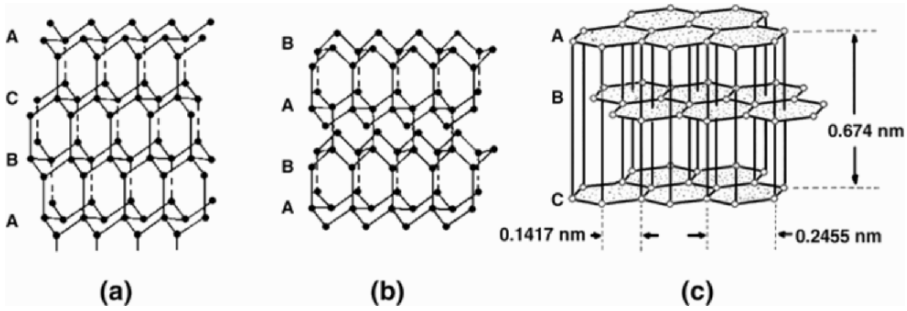

Figure 6-18. Crystal structure of graphite. Reprinted with permission from Shobert (1964). Copyright © 1964, Academic Press.

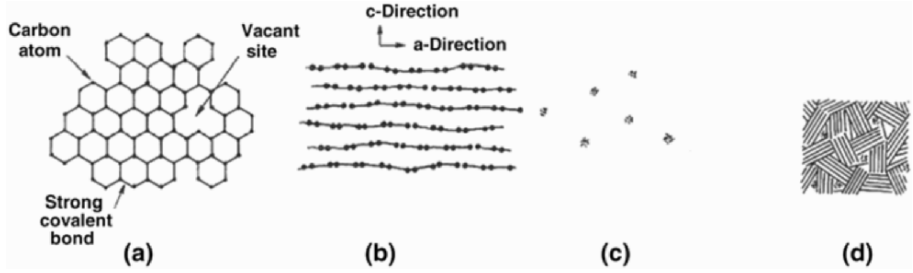

Figure 6-19. Schematic representation of poorly crystalline carbon: (**a**) single-layer plane; (**b**) parallel layers in a crystalline; (**c**) unassociated carbon; (**d**) an aggregate of crystallites, single layers and unassociated carbon. Reprinted with permission from Bokros (1972). Copyright © 1972, Marcel Dekker.

6.7.2. Properties of Carbon

The mechanical properties of carbon, especially pyrolytic carbon, are largely dependent on density, as shown in Figures 6-20 and 6-21. The increased mechanical properties are directly related to the increased density, which indicates the properties depend mainly on the aggregate structure of the material.

Graphite and glassy carbon have much lower mechanical strength than pyrolytic carbon, as given in Table 6-11. However, the average modulus of elasticity is almost the same for all carbons. The strength of pyrolytic carbon is quite high compared to graphite and glassy carbon. This is again due to the lesser amount of flaws and unassociated carbons in the aggregate.

A composite carbon that is reinforced with carbon fiber has been considered for implants. The properties are highly anisotropic, as given in Table 6-12. The density is in the range of 1.4–1.45 g/cm^3, with a porosity of 35–38%.

Carbons exhibit excellent compatibility with tissues. In particular, compatibility with blood has made pyrolytic carbon deposited heart valves and blood vessel walls a widely accepted part of the surgical armamentarium.

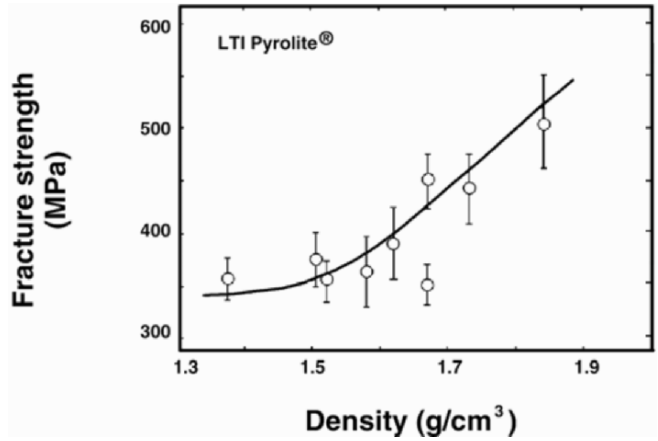

Figure 6-20. Fracture stress versus density for unalloyed LTI pyrolite carbons. Reprinted with permission from Kaae (1971). Copyright © 1971, Elsevier Science.

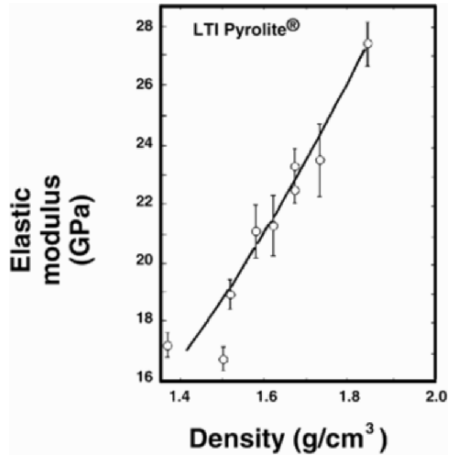

Figure 6-21. Elastic moduli versus density for unalloyed LTI pyrolite carbons. Reprinted with permission from Kaae (1971). Copyright © 1971, Elsevier Science.

6.7.3. Manufacture of Implants

Pyrolytic carbons can be deposited onto finished implants from hydrocarbon gas in a *fluidized bed* at a controlled temperature and pressure, as shown in Figure 6-22. The anisotropy, density, crystallite size, and structure of the deposited carbon can be controlled by temperature, composition of the fluidizing gas, bed geometry, and residence time (velocity) of the gas molecules in the bed. The microstructure of deposited carbon should be particularly controlled since the formation of growth features associated with uneven crystallization can result in a weaker material, as shown in Figure 6-23. It is also possible to introduce various other elements into the fluidizing gas and codeposit them with carbon. Usually silicon (10–20 w/o) is codeposited (or

alloyed) to increase hardness for applications requiring resistance to abrasion, such as heart valve discs.

Table 6-11. Properties of Various Types of Carbon

	Types of carbon		
Properties	Graphite	Glassy	Pyrolytica
Density (g/cm^3)	1.5-1.9	1.5	1.5-2.0
Elastic modulus (GPa)	24	24	28
Compressive strength (MPa)	138	172	517 (575[a])
Toughness (mN/cm^3)[b]	6.3	0.6	4.8

[a] 1.0 w/o Si-alloyed pyrolytic carbon, Pyrolite® (Carbomedics, Austin, TX)
[b] 1 m-N/cm^3 = 1.45×10^{-3} in-lb/in^3.

Table 6-12. Mechanical Properties of Carbon Fiber-Reinforced Carbon

	Fiber lay-up	
Property	Unidirectional 0–90º	Crossply
Flexural modulus (GPa)		
Longitudinal	140	60
Transverse	7	60
Flexural strength (MPa)		
Longitudinal	1,200	500
Transverse	15	500
Interlaminar shear strength (MPa)	18	18

Pyrolytic carbon was deposited onto the surfaces of blood vessel implants made of polymers. This is called ultra-low-temperature isotropic (ULTI) carbon, instead of LTI (low-temperature-isotropic) carbon. The deposited carbon is thin enough not to interfere with the flexibility of grafts yet exhibits excellent blood compatibility.

The vitreous or glassy carbon is made by controlled pyrolysis of polymers such as phenolformaldehyde, rayon (Glasser et al., 1992), and polyacrylonitrile at high temperature in a controlled environment. This process is particularly useful for making carbon fibers and textiles, which can themselves be used or as components of composites.

6.8. DETERIORATION OF CERAMICS

It is of great interest to know whether inert ceramics such as alumina undergo significant static or dynamic fatigue. In one study it was shown that above a critical stress level the fatigue strength of alumina is reduced by the presence of water. This is due to delayed crack growth, which is accelerated by the water molecules. However, another study showed that a reduction in strength occurred if evidence of penetration by water was observed under a scanning electron microscope (SEM). No decrease in strength was observed for samples that showed no watermarks on the fractured surface, as shown in Figure 6-24. It was suggested that the presence of a minor amount of silica in one sample lot may have contributed to permeation of the

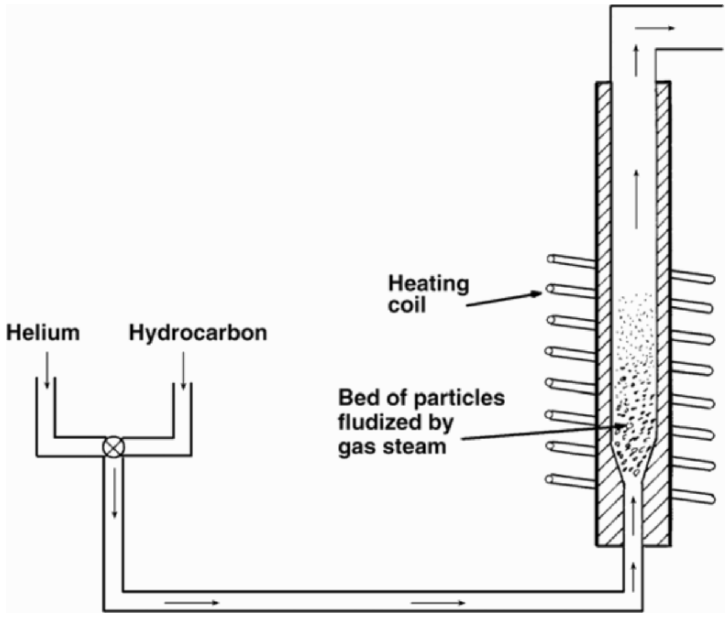

Figure 6-22. Schematic diagram showing particles being coated with carbon in a fluidized bed. Reprinted with permission from Bokros (1972). Copyright © 1972, Marcel Dekker.

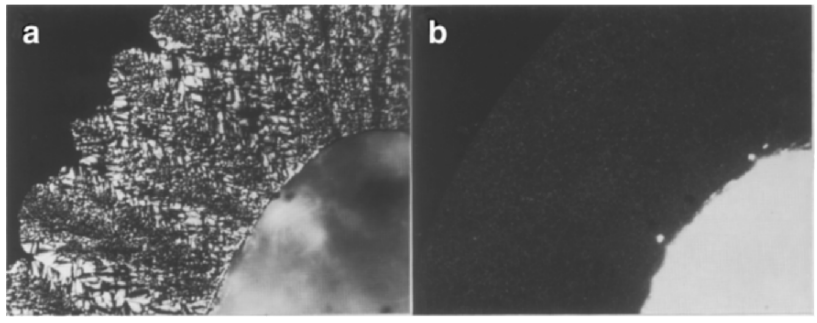

Figure 6-23. Microstructures of carbons deposited in a fluidized bed: (**a**) granular carbon with distinct growth features; (**b**) isotropic carbon without growth features. Both under polarized light, 240×. Reprinted with permission from Bokros (1972). Copyright © 1972, Marcel Dekker.

water molecules, which is detrimental to strength. It is not clear whether the same static fatigue mechanism operates in single-crystal alumina or not. It is, however, reasonable to assume that the same static fatigue will occur if the ceramic contains flaws or impurities, which will act as the source of crack initiation and growth under stress.

A study of the fatigue behavior of vapor-deposited pyrolytic carbon fibers (400–500 nm thick) onto a stainless steel substrate showed that the film did not break unless the substrate

underwent plastic deformation at 1.3×10^{-2} strain and up to one million cycles of loading. Therefore, the fatigue is closely related to the substrate, as shown in Figure 6-25. A similar substrate–carbon adherence is the basis for the pyrolytic carbon-deposited polymer arterial grafts, as mentioned earlier.

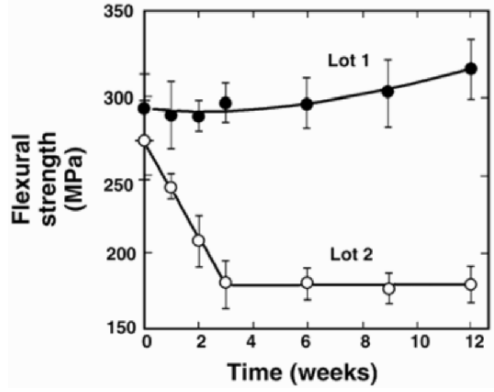

Figure 6-24. Flexural strength of dense alumina rods after aging under stress in Ringer's solution base indicating standard deviation. Lots 1 and 2 are from different batches of production. Reprinted with permission from Krainess and Knapp (1978). Copyright © 1978, Wiley.

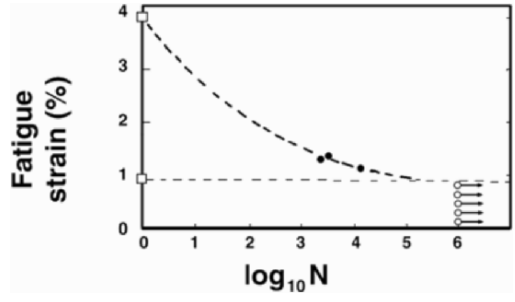

Figure 6-25. Strain versus number of cycles to failure: ○ = absence of fatigue cracks in carbon film; ● = fracture of carbon film due to fatigue failure of substrates; □ = data for substrate determined in single-cycle tensile test. Reprinted with permission from Shim and Haubold (1980). Copyright © 1980, Marcel Dekker.

The fatigue life of ceramics can be predicted by assuming that fatigue fracture is due to the slow growth of preexisting flaws. Generally, the strength distribution (s_i) of ceramics in an inert atmosphere can be correlated with the probability of failure F, by the following equation;

$$\ln \ln \left(\frac{1}{1-F} \right) = m \ln \left(\frac{s_i}{s_0} \right), \tag{6-3}$$

in which m and s_0 are constants. The m is called the Weibull modulus, which indicates the distribution of fracture strength: the higher the value, the narrower the distribution. The metals and polymers have values of 50, while most ceramics and glasses have values less than 20. Figure 6-26 shows a good fit for Bioglass®-coated alumina.

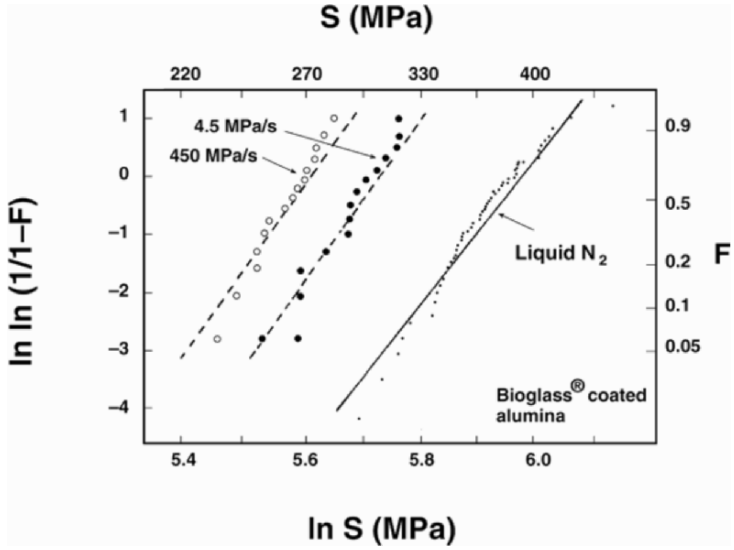

Figure 6-26. Plot of ln [1/(1 – F)] versus ln s for Bioglass®-coated alumina in a tris hydroxyaminomethane buffer and liquid nitrogen. F is the probability of failure and σ is strength. Reprinted with permission from Ritter et al. (1979). Copyright © 1979, Wiley.

A minimum service life (t_{min}) of a specimen can be predicted by means of a proof test wherein it is subjected to stresses greater than those expected in service. Proof tests also eliminate weaker pieces. This minimum life can be predicted from the following equation:

$$t_{\min} = B\sigma_p^{N-2}\sigma_a^{-N}, \tag{6-4}$$

in which σ_P is the proof test stress, σ_a is the applied stress, and B and N are constants. Rearranging Eq. (6-3), we obtain

$$t_{\min}\sigma_a^2 = B\left(\frac{\sigma_p}{\sigma_a}\right)^2. \tag{6-5}$$

Figure 6-27 shows a plot of Eq. (6-5) for alumina on a logarithmic scale.

Example 6-6

Calculate the proof stress of an alumina sample if it is to last for 20 years at 100 MPa in air and in Ringer's solution.

Answer

$$t_{\min}\sigma_a^2 = 20 \text{ yr} \times 3.15 \times 10^7 \text{ s/yr} \times (100 \text{ MPa})^2,$$

$$\log t_{\min}\sigma_a^2 = 12.8.$$

This value is comparable to the dotted line for 80 years at 69 MPa in Figure 6-27. Therefore, $\sigma_p/\sigma_a = 2.0$ in air and 2.55 in Ringer's solution. So σ_p = 200 MPa in air, and σ_p = 255 MPa in Ringer's solution. As one might expect, it is necessary to test the sample more rigorously in Ringer's solution than in air.

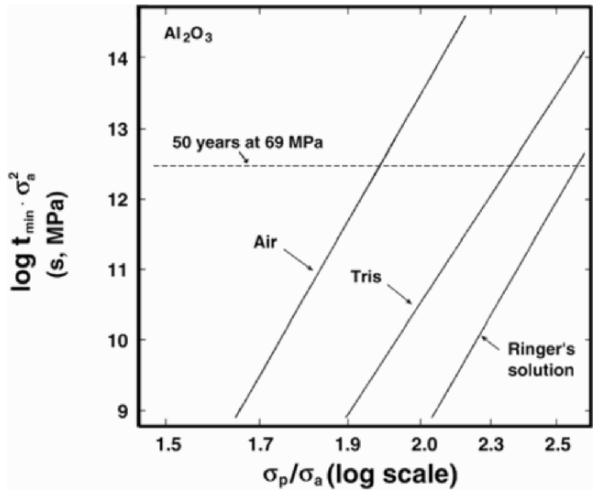

Figure 6-27. Plot of Eq. (6-45) for alumina after proof testing. N = 43.85, m = 13.21, and σ_0 = 55,728 psi. Reprinted with permission from Ritter et al. (1979). Copyright © 1979, Wiley.

PROBLEMS

6-1. A ceramic is used to fabricate a hip joint. Assume a simple ball-and-socket configuration with a surface contact area of 1.0 cm^2 and continuous static loading in a simulated condition similar to Figure 6-17 (extrapolate the data if necessary). Observe that the actual contact area is smaller than the total surface area.

a. How long will it last if the loading is a force due to 70 kg (mass), in water and in blood?

b. Will the implant last a longer or shorter time with dynamic loading? Give reasons.

6-2. From the phase diagram of Al_2O_3–SiO_2,

a. Determine the exact mole % of Al_2O_3–SiO_2 for mullite, which has a $3Al_2O_3$–$2SiO_2$ composition.

b. Determine the amount of mullite in 50 wt % Al_2O_3–50 wt% SiO_2 at 1469ºC.

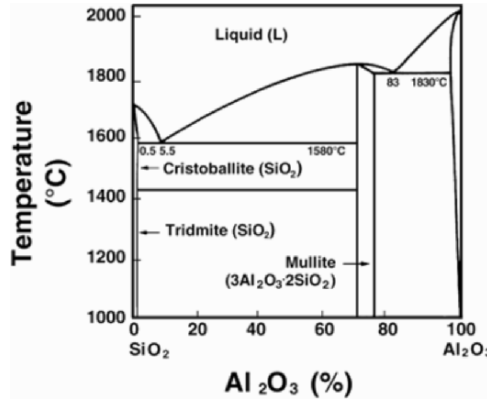

6-3. Calculate the proof stress of an alumina sample if it is to last for 40 years at 100 MPa in air and in Ringer's solution.

6-4. One is trying to coat the surface of an orthopedic implant with hydroxyapatite to enhance compatibility with tissues. List the possible problems associated with this technique. Give two methods of applying the coating.

6-5. Discuss the advantages of coating the femoral stem of a hip prosthesis with hydroxyapatite, alumina, and diamond-like carbon. Give two general advantages to all ceramic coatings and, in addition, one or more specific advantage(s) for each coating. Show them in table form.

6-6. Zirconia (ZrO_2) is often stabilized with calcium to provide an important refractory. The basic cell is ZrO_2 with 1 Ca^{2+} ion present for every 10 Zr^{4+} ions. Will the vacant sites be anion or cation? What percentage of the total number of all sites will be vacant?

6-7. Calculate the density of monoclinic and tetragonal zirconia.

6-8. Calculate the amount of volume change when the zirconia changes from monoclinic to tetragonal structure.

6-9. Calculate the amount of volume change by adding 3 mole% of Y_2O_3 into cubic zirconia. Make assumptions of ideal mixing.

6-10. Consider the following mechanical properties.

Properties	Bone	Vitreous carbon
Ultimate tensile strength (MPa)	100	120
Tensile modulus (GPa)	12–18	2.8

This comparison suggests that vitreous carbon would be an excellent material for bone replacement. What is wrong with this idea?

6-11. Discuss the advantages of coating the femoral stem of a hip prosthesis with hydroxyapatite, alumina, and diamond-like carbon. Give two general advantages to all ceramic coatings and, in addition, one or more specific advantage(s) for each coating. Show them in a table form.

6-12. CsCl has a simple cubic structure and the following data are given:

Element	Ion radius (nm)	amu
Cl	0.181	35.4
Cs	0.165	132.9

a. Calculate the minimum radius ratio of a simple cubic cell.

b. What is the coordination number of the Cs?

c. What is the density of CsCl?

d. Why is this material brittle?

6-13. NaCl has a face-centered cubic structure and the following data are given:

Element	Ion radius (Å)	amu
Cl	1.81	35.4
Na	0.97	23

a. Draw the positions of Cl and Na ions in one of the cubic faces.

b. What is the coordination number of the Na?

c. Calculate the lattice parameter (a) of the unit cell.

d. Calculate the density of NaCl.

f. Which direction will have the highest linear density of ions: [100], [110], or [111]?

e. Why is this material brittle?

6-14. From the list of ceramics choose the most appropriate one:

A. Al_2O_3 B. Hydroxyapatite C. Tricalcium phosphate
D. Carbon E. Glass-ceramic

a. Resorbable in vivo.

b. Has best blood compatibility

c. A large single crystal can be made and sometimes is called ruby or sapphire

d. Has a direct bone-bonding ability

e. Bone mineral has the similar structure

6-15. From the following ceramic materials select the most appropriate one for the questions:

A. Al_2O_3 B. $Ca_3(PO_4)_2$ C. $Ca_{10}(PO_4)_6(OH)_2$ D. 45S5
E. LTI F. ZrO_2 G. DLC

a. Osteogenic properties.

b. Used to make dental implants.

c. Hardest ceramic among those listed.

d. β-whitlockite forms in dry condition.

e. Readily resorbed in vivo.

f. AmXn structure and 2/3 available lattice sites are filled.

g. Fluidized bed is used to coat the surface of heart valve discs.

h. Glass ceramic and has capacity to bond directly with bone.

i. Similar to the diamond, coated on a surface.

j. Single crystal is used for making jewels.

6-16. Collagen and TGF-β (tissue growth factor) are mixed with hydroxyapatite (Ha et al., 1993) for making synthetic bone [BioME®] implants. A 10-mm diameter 20-mm long BioME® rod is made using 49–49–2% by weight [2% is TGF-β] of the materials to test its properties. Using the following data, answer the following questions:

Material	Young's modulus (GPa)	Strength (MPa)	Density (g/cc)
Collagen	1	10 (yield)	1.0
HA	100	100 (fracture)	3.2
TGF-β	0	0	1.0

a. Calculate the density of the BioME®.

b. Calculate the yield strain of the BioME®.

c. Calculate the Young's modulus of the BioME®.

d. Calculate the maximum strength of the BioME®.

e. Give at least one reason why you would *not* use TGF-β to make the BioME®.

SYMBOLS/DEFINITIONS

Words

Activation energy of phase transformation: Thermal energy required to overcome an energy barrier. $E_{activation} = RT$ ln(transformation rate), where R is the gas constant and T is temperature (K).

Alumina: Aluminum oxide (Al_2O_3), which is very hard (Mohs hardness of 9) and strong. Single crystals are called sapphire or ruby depending on color. Alumina is used to fabricate hip joint socket components or dental root implants.

Baddeleyite: Mineral containing zircon.

Biolox®: Trade name of alumina ceramic.

Calcium phosphate: A family of calcium phosphate ceramics including hydroxyapatite β-whitlockite, mono-, di-, tri-, and tetra-calcium phosphate, which are used to make substitute or augment artificial bone substitutes.

Cubic zirconia: Partially stabilized zirconia in cubic structure to prevent fracture during cooling.

Electronegativity: Potential of an atom to attract electrons, especially in the context of forming a chemical bond.

Fluorite (CaF_2) structure: AX_2 structure of ceramic, where A is a metal and X a nonmetal.

Glass-ceramics: A glass crystallized by heat treatment. Some of those have the ability of forming chemical bonds with hard and soft tissues. Bioglass® and Ceravital® are well-known examples.

Hydroxyapatite [$Ca_{10}(PO4)_6(OH)_2$]: A calcium phosphate ceramic with a calcium-to-phosphorus ratio of 5/3 and nominal composition. It has good mechanical properties and excellent biocompatibility. Hydroxyapatite is the mineral constituent of bone.

LTI carbon: A silicon alloyed pyrolytic carbon deposited onto a substrate at low temperature with isotropic crystal morphology. Highly blood compatible and used for cardiovascular implant fabrication, such as artificial heart valves.

Maximum radius ratio: The ratio of atomic radii computed by assuming the largest atom or ion which can be placed in a crystal's unit cell structure without deforming the structure.

Mohs scale: A hardness scale in which 10 (diamond) is the highest and 1(talc) is the softest.

Monoclinic structure: One crystal system having $a \neq b \neq c$, $\alpha = \gamma = 90^\circ$.

Partially stabilized zirconia: See cubic zirconia.

Phase transformation toughening process: By transforming phases under stress the material becomes stronger due to the volume expansion of the transformed phase.

Tetragonal structure: One crystal system having $a = b \neq c$, $\alpha = \beta = \gamma = 90^\circ$.

Wear factor: Similar to the wear constant; wear volume generated by given load and sliding distance .

Weibull modulus: Slope of the Weibull plot. Larger values indicate predictable failure stress. Ceramics are 10~20, metals are >50.

Weibull plot: Plot of the logarithm of probability of failure (F) [actually, $\ln \ln 1/(1 - F)$] and test stress/strength fraction.

β-whitlockite ($3CaO \cdot P_2O_3$): One of the calcium phosphate compounds, similar to tricalcium phosphate, $3Ca \cdot PO_4$.

Yttrium oxide (Y_2O_3): Oxide used to partially stabilize zirconia.

Zircon ($ZrSiO_4$): Crystalline mineral, a silicate of zirconium with tetragonal structure.

Zirconia (ZrO_2): Zirconium oxide, which is hard and strong.

BIBLIOGRAPHY

Adams D, Williams DF. 1978. Carbon fiber-reinforced carbon as a potential implant material. *J Biomed Mater Res* **12**:35–42.

ASTM. 2000. *Annual book of ASTM standards*. West Conshohocken, PA: ASTM.

Beckham CA, Greenlee Jr TK, Crebo AR. 1971. Bone formation at a ceramic implant interfacing. *Calcif Tissue Res* **8**:165–171.

Blencke BA, Bromer H, Deutscher KK. 1978. Compatibility and long-term stability of glass-ceramic implants. *J Biomed Mater Res* **12**(3):307–316.

Bokros JC, LaGrange LD, Schoen GJ. 1972. Control of structure of carbon for use in bioengineering. In *Chemistry and physics of carbon*, pp. 103–171. Ed PL Walker. New York: Dekker.

Bokros JC, Atkins RJ, Shim HS, Haubold AD, Agarwal MK. 1976. Carbon in prosthetic devices. In *Petroleum derived carbons*, pp. 237–265. Ed ML Deviney, TM O'Grady. Washington, DC: American Chemical Society.

Burger W, Willmann G. 1993. Advantages and risks of zirconia ceramics in biomedical applications. In *Bioceramics*, Vol. 6, pp. 299-304. Ed P Ducheyne, D Christiansen. Oxford: Pergamon.

Callister JWD. 1994. *Materials science and engineering: an introduction*, 3rd ed. New York: Wiley.

Drennan J, Steele BCH. 1986. Zirconia and hafnia. In *Encyclopedia of materials science and engineering*, pp. 5542–5545. Ed MB Beaver. Oxford: Pergamon/MIT Press.

Gill RM. 1972. *Carbon fibres in composite materials*. London: Butterworths.

Gilman JJ. 1967. The nature of ceramics. *Sci Am* **218**(3):113.

Gitzen WH, ed. 1970. *Alumina as a ceramic material*. Westerville, OH: American Ceramic Society.

Glasser WG, Hatakeyama H, eds. 1992. *Viscoelasticity of biomaterials*. Washington, DC: American Chemical Society.

Ha S-W, Mayer J, Wintermantel E. 1993. Micro-mechanical testing of hydroxyapatite coatings on carbon fiber reinforced thermoplastics. In *Bioceramics*, Vol. 6, 489–493. Ed P Ducheyne, D Christiansen. Oxford: Pergamon.

Hastings GW, Williams, DF, eds. 1980. *Mechanical properties of biomaterials*, Part 3. Chichester: Wiley.

Hench LL, Ethridge EC. 1982. *Biomaterials: an interfacial approach*. New York: Academic Press.

Horwitz BR, Rockowitz NL, Goll SR, Booth Jr RE, Balderston RA, Rothman RH, Cohn JC. 1993. A prospective randomized comparison of two surgical approaches to total hip arthroplasty. *Clin Orthop Relat Res* **291**:154–163.

Hulbert SF, Young FA, eds. 1978. *Use of ceramics in surgical implants*. New York: Gordon & Breach.

Hulbert SF, King FW Jr, Klawitter JJ. 1972. Initial surface interaction of blood and blood components with Al_2O_3 and TiO_2. *J Biomed Mater Res Symp* **2**:69–89

Kaae JL. 1971. Structure and mechanical properties of isotropic pyrolytic carbon deposited below 1600 degrees. *J Nucl Mater* **38**:42–50.

Kawahara H, Hirabayashi M, Shikita T. 1980. Single crystal alumina for dental implants and bone screws. *J Biomed Mater Res* **14**:597–606.

Kingery WD, Bowen HK, Uhlmann DR. 1976. *Introduction to ceramics*, 2nd ed. New York: Wiley.

Krainess FE, Knapp WJ. 1978. Strength of a dense alumina ceramic after aging in vitro. *J Biomed Mater Res* **12**:241–246.

Kumar P, Shimizu K, Oka M. 1991. Low wear rate of UHMWPE against zirconia ceramic (Y-PSZ) in comparison to alumina ceramic and SUS 316L alloy. *J Biomed Mater Res* **25**:813–828.

McConell D. 1973. *Apatite: its crystal chemistry, mineralogy, utilization, and biologic occurrence*. Berlin: Springer-Verlag.

McMillan PW. 1979. *Glass-ceramics*. New York: Academic Press.

Niwa S, Sawai K, Takahashie S, Tagai H, Ono M, Fukuda Y. 1980. Experimental studies on the implantation of hydroxyapatite in the medullary canal of rabbits. In *Proceedings of the first world biomaterials congress* (Baden, Austria). Berlin: Springer-Verlag.

Norton F. 1974. *Elements of ceramics*. Reading, MA: Addison-Wesley.

Ogino M, Ohuchi F, Hench LL. 1980. Compositional dependence of the formation of calcium phosphate film on Bioglass. *J Biomed Mater Res* **14**:55–64.

Posner AS, Perloff A, Diorio AD. 1958. Refinement of the hydroxyapatite structure. *Acta Crystallogr* **11**:308–309.

Ritter Jr JE, Greenspan DC, Palmer RA, Hench LL. 1979. Use of fracture of an alumina and Bioglass-coated alumina. *J Biomed Mater Res* **13**:251–263.

Schnittgrund GS, Kenner GH, Brown SD. 1973. In vivo and in vitro changes in strength of orthopedic calcium aluminate. *J Biomed Mater Res Symp* **4**:435–452.

Shim HS, Haubold AD. 1980. The fatigue behavior of vapor deposited carbon films. *Biomater Med Devices Artif Organs* **8**:333–344.

Shimizu K, Oka M, Kumar P, Kotoura Y, Yamamuro T, Makinouchi K, Nakamura T. 1993. Time-dependent changes in the mechanical properties of zirconia ceramic. *J Biomed Mater Res* **27**:729–734.

Shobert EI. 1964. *Carbon and graphite*. New York: Academic Press.

Starfield MJ, Shrager AM. 1972. *Introductory to materials science*. New York: McGraw-Hill.

Willmann G. 1993. Zirconia: a medical-grade material? In *Bioceramics*, Vol. 6. pp. 271–276. Ed P Ducheyne, D Christiansen. Oxford: Pergamon.

Yoshimura M, Suda H, eds. 1994. *Hydrothermal processing of hydroxyapatite: past, present, and future. Hydroxyapatite and related materials*. Boca Raton, FL: CRC Press.